

# Physical Damage on Giant Vesicles Membrane as a Result of Methylene Blue Photoirradiation

Omar Mertins,<sup>†\*</sup> Isabel O. L. Bacellar,<sup>‡</sup> Fabrice Thalmann,<sup>§</sup> Carlos M. Marques,<sup>§</sup> Maurício S. Baptista,<sup>‡</sup> and Rosangela Itri<sup>†\*</sup>

<sup>†</sup>Departamento de Física Aplicada, Instituto de Física, Universidade de São Paulo; <sup>‡</sup>Departamento de Bioquímica, Instituto de Química, Universidade de São Paulo, São Paulo, Brazil; and <sup>§</sup>Institut Charles Sadron, Université de Strasbourg, Centre National de la Recherche Scientifique, Strasbourg, France

**ABSTRACT** In this study we pursue a closer analysis of the photodamage promoted on giant unilamellar vesicles membranes made of dioleoyl-*sn*-glycero-3-phosphocholine (DOPC) or 1-palmitoyl-2-oleoyl-*sn*-glycero-3-phosphocholine (POPC), by irradiating methylene blue present in the giant unilamellar vesicles solution. By means of optical microscopy and electro-deformation experiments, the physical damage on the vesicle membrane was followed and the phospholipids oxidation was evaluated in terms of changes in the membrane surface area and permeability. As expected, oxidation modifies structural characteristics of the phospholipids that lead to remarkable membrane alterations. By comparing DOPC- with POPC-made membranes, we observed that the rate of pore formation and vesicle degradation as a function of methylene blue concentration follows a diffusion law in the case of DOPC and a linear variation in the case of POPC. We attributed this scenario to the nucleation process of oxidized species following a diffusion-limited growth regime for DOPC and in the case of POPC a homogeneous nucleation process. On the basis of these premises, we constructed models based on reaction-diffusion equations that fit well with the experimental data. This information shows that the outcome of the photosensitization reactions is critically dependent on the type of lipid present in the membrane.

## INTRODUCTION

The biophysics of biological membranes is forsooth affected by oxidative stress resulting in a variety of the cell responses that are dependent on biochemical, pathological, and environmental conditions (1–3). Among the diversity of studies, peroxidation of the lipids that compose the membrane has received recognition as one of the key factors that eventually lead to cell apoptosis/necrosis (3–7). In this sense, it has been shown that photoactive molecules, when excited with the appropriate irradiation, may transfer their energy to molecular oxygen. Consequently, highly reactive singlet oxygen <sup>1</sup>O<sub>2</sub> and/or free radicals (known as reactive oxygen species) are generated which, in turn, promote oxidative reactions, altering the molecular structure of unsaturated lipids. Thereby, modifications in the membrane properties such as permeability, headgroup hydration, fluidity, and packing order are expected (8–13). Therefore, the oxidative stress that results from the action of reactive oxygen species may lead to severe physical damage on biological membranes and the extent of dysfunctions may cause cell death.

In mammals, the *sn*-2 position of diacyl glycerophospholipids is frequently linked to polyunsaturated fatty acids that are prone to oxidative modification (3). Two classes of oxidized glycerophospholipids have been mainly studied in the literature: hydroxyl- or hydroperoxy-dienoyl phosphatidylcholines and phosphatidylcholines with oxidized and truncated chains with either aldehyde or the carboxylic

group (7,11,12). The biophysical changes of membranes are indeed related to the molecular characteristics and concentrations of the oxidized lipids (13,14).

The membrane response to oxidative stress is the base of photodynamic therapy, especially in applying photosensitizer molecules that have specificity and preferential interaction with tumor tissues. Methylene blue (MB) has been clinically applied as a photosensitizer molecule to treat Kaposi's sarcoma (15), herpes (16), and in antimicrobial chemotherapy (17). It has been previously shown that MB has affinity to mitochondria (18), resulting in cell apoptosis and thus minimizing the inflammatory response (19), although its mechanism of action on membranes is still unclear. MB features important photochemical characteristics such as high quantum yield of singlet oxygen production besides the possibility to generate several radical species through type II and type I mechanisms, respectively (20,21).

Previous reports described the photodamage promoted in giant unilamellar vesicles (GUVs) and changes in the lipids molecular structure were proposed (22–24). The irradiation of GUVs of 1,2-dioleoyl-*sn*-glycero-3-phosphocholine (DOPC) dispersed in aqueous solution of MB at concentrations >40 μMolar promoted disruption of the membrane (22). Such an effect was associated with photochemical reactions started by the singlet oxygen attack to the double bonds of the two acyl tails thus producing lipid hydroperoxides (25). In the absence of metal ions in solution, the auto-catalytic peroxidation reactions may proceed in the presence of a type I photosensitizer, such as MB, generating shortened acyl chains (26) which, by turn, destabilize the membrane (22). On the other hand, the photo-induced effect of

Submitted May 25, 2013, and accepted for publication November 18, 2013.

\*Correspondence: mertins@if.usp.br or itri@if.usp.br

Editor: Reinhard Lipowsky.

© 2014 by the Biophysical Society  
0006-3495/14/01/0162/10 \$2.00

<http://dx.doi.org/10.1016/j.bpj.2013.11.4457>



a new porphyrin derivative, with high efficiency of singlet oxygen production, incorporated into GUVs of 1-palmitoyl-2-oleoyl-*sn*-glycero-3-phosphocholine (POPC) with just one unsaturated acyl chain, propelled morphological changes of the vesicles driven by an increase in the surface area (23). Such an area increase was attributed to the accumulation of POPC hydroperoxides in the membrane as a by-product from the  $^1\text{O}_2$  reaction to the chain double bond of POPC. Interestingly, neither membrane disruption nor increase in permeability was observed even when a massive amount of lipid hydroperoxides was present in the membrane (23). It is further known by fluorescence correlation spectroscopy that the presence of oxidized lipids leads to an increase in the headgroup hydration and mobility and faster lipid lateral diffusion in POPC membranes (11). Interestingly, the presence of oxidized lipids can also promote phase separation on binary (27) and ternary lipid mixtures (28). However, very few fundamental questions related to the molecular structure of the lipids have been answered so far. For example, how different DOPC or POPC membranes respond to the oxidative stress induced by the photosensitization reaction remains an open question.

To better understand how the photodamage on the membrane depends on the phospholipid structure, a closer analysis of the rate of damage promoted by irradiation of MB on GUVs composed either by DOPC or by POPC lipids, which are lipids that differ by one saturated acyl chain, was undertaken in this study. As published before by us as well as by others, the morphological changes on the vesicles are remarkable. However, total destruction of the membrane is avoided in this study by means of time-controlled experiments. Different from other reports, the physical damages on the vesicle membranes were evaluated by taking into account the increase of membrane surface area, sucrose, and NaCl permeability increase. This comprehensive strategy, allowed for a precise comparison of the differences between DOPC and POPC membranes, an effect that could be modeled by using diffusion-reaction equations.

## MATERIALS AND METHODS

### Materials

Stock solutions of the POPC and DOPC from Avanti Polar Lipids (Birmingham, AL) were prepared in chloroform (99.8%; Synth, Diadema, Brazil). MB was purchased from Sigma-Aldrich and all stock solutions were prepared in purified water. The MB molar concentration was checked using a spectrophotometer (Ocean Optics USB-2000; Dunedin, FL) by taking into account the molar extinction coefficient of 81600 at  $\lambda = 664$  nm. Sucrose (99%; Sigma-Aldrich), glucose (99%; Sigma-Aldrich, St. Louis, MO), and all other reagents were of analytical grade.

### MB binding to POPC and DOPC membranes

Lipid films containing ~30 mg of DOPC or POPC were prepared by the evaporation of chloroform solutions in glass tubes. These were hydrated with 1 mL of Milli-Q water, and then vortexed and sonicated. To isolate the

heavier liposomes, the resulting liposome suspensions were transferred to Eppendorf tubes and subjected to two steps: i), centrifugation for 5 min at 13,000 rpm and ii), removal of the supernatant, followed by dissolution of the pellet in 1 mL of Milli-Q water. The sequence composed by steps (i) and (ii) was repeated three times. To quantify the binding of MB to the liposomes, 300  $\mu\text{L}$  of the heavier liposomes suspensions were added to Eppendorf tubes containing 13  $\mu\text{M}$  MB in Milli-Q water (after addition of liposomes, MB concentration fell to 10  $\mu\text{M}$ ). After 10 min of incubation, these tubes were centrifuged for 5 min at 13,000 rpm. Because the interaction of MB with neutral membranes is very low, it was not possible to measure changes in MB concentration in the aqueous solution. Instead, measurements were done using only the lipid pellet. The supernatant was removed with a pipette, and the pellet was dissolved in 1 mL of a 90 mM SDS solution with 10% of Triton X-100. The absorption spectrum of this solution was obtained in the 400–800 nm range, using a Shimadzu UV-2400-PC spectrophotometer (Kyoto, Japan) and a quartz cuvette of 1 cm optical path. The absorption at 538 nm was subtracted from all spectra, and the concentration of MB in the solution was estimated using the absorbance at 662 nm (absorption maximum in this condition) and the molar absorptivity coefficient for MB in ethanol (81600  $\text{M}^{-1} \text{cm}^{-1}$ ). We assumed that all MB molecules in the pellet were retained by interaction with the membranes. Hence, the calculated concentration was taken as the concentration of MB bound to lipids ([MB-L]) in the binding equilibrium  $\text{MB} + \text{L} \rightleftharpoons \text{MB-L}$ , where L means lipids from the membranes. This equilibrium can be translated into a binding constant  $K_b = [\text{MB-L}]/([\text{MB}][\text{L}])$ . To obtain the value of  $K_b$ , the concentration of MB in the supernatant ([MB]) was calculated by  $10 \mu\text{M} - [\text{MB-L}]$  and the lipid concentration in the pellet ([L]) was determined colorimetrically (29). The reported  $K_b$  values are in the form of mean  $\pm$  standard deviation ( $n = 8$  and 9 for DOPC and POPC, respectively). Three different lipid films were prepared and used to obtain independent triplicates for each lipid.

### Preparation of GUVs

GUVs of POPC or DOPC were prepared using the traditional electroformation method (30). Briefly, 10  $\mu\text{L}$  of a 2 mM lipid solution in chloroform were spread onto the surfaces of two conductive glasses (coated with Fluor Tin Oxide), which were then placed with their conductive sides facing each other separated by a 2 mm thick Teflon frame. This electro swelling chamber was filled with 0.2 M sucrose solution and branched to an alternating power generator (Minipa MFG-4201A; Korea) at 1.5 V and 10 Hz frequency during 2 h at room temperature (22–24°C). The vesicles solution was then carefully transferred to an Eppendorf vial and kept at rest at 4°C before use. A typical observation experiment, using an inverted microscope (see below), was made in an observation chamber by mixing 50  $\mu\text{L}$  of the GUVs solution with 300  $\mu\text{L}$  of a 0.2 M glucose solution. This created a sugar asymmetry between the interior and the exterior of the vesicles. The osmolarities of the sucrose and glucose solutions were measured with a cryoscopic osmometer Osmomat 030 (Gonotec; Berlin, Germany) and carefully matched to avoid osmotic pressure effects. The slight densities difference between the inner and outer solutions drive the vesicles to the bottom slide where they can easily be observed and in addition, the refractive index difference between sucrose and glucose solutions provides a better contrast when observing the vesicles with phase contrast microscopy.

For the experiments with photodamage of the vesicles membrane, different concentrations of MB were previously dissolved in the glucose solution and the procedure described previously was followed. The concentrations of MB (10, 20, 30, and 40  $\mu\text{M}$ ) were calculated for the final solutions in the observation chamber.

### Optical microscopy observation, irradiation, and electro-deformation

We used an inverted microscope Axiovert 200 (Carl Zeiss; Jena, Germany) with a Ph2 63 $\times$  objective. Images were recorded with an AxioCam HSm

digital camera (Carl Zeiss). The illumination system of the microscope was used in the transmission mode (bright field), with low intensity illumination, to observe the vesicles. Under these conditions no perturbation of the vesicles in the presence of MB occurred over 1 h of observation. Irradiation of the samples was performed with the 103W Hg lamp (HXP 120, Kubler, Carl Zeiss, Jena, Germany) of the microscope using an appropriate filter for photoactivation of MB ( $\lambda_{\text{ex}} = 665 \text{ nm}$ ;  $\lambda_{\text{em}} = 725 \text{ nm}$ ).

The experiments of electro-deformation were performed by submitting the samples to an alternating electrical (AC) field of 10 V intensity and 1 MHz frequency (23,31). In this case, the vesicles were grown in the sucrose solution containing a small amount of salt (0.5 mM NaCl) to ensure a higher conductivity inside, and thus to induce prolate deformation (32) followed by dilution in a MB-containing glucose solution. The GUVs solution was then placed into a special chamber purchased from Eppendorf (Hamburg, Germany), which consists of an 8 mm thick Teflon frame confined between two glass plates through which observation was possible. A pair of parallel platinum electrode wires with 90  $\mu\text{m}$  in radius was fixed to the lower glass. The gap distance between the two wires was 0.5 mm. The chamber was branched to a function generator and the vesicles lying between the two parallel wires were observed.

## RESULTS

### Giant vesicles photodamage

Photodamage on biological membranes promoted by MB may have different levels and characteristics depending particularly on MB concentration. It is worth noting that only singlet oxygen produced in the vicinity of the phospholipid bilayer (around 100 nm) is able to interact with the membrane due to its short life time in aqueous solution (22). In this study, we noticed by optical microscopy a small adsorption of MB to PC-based lipids as evidenced by a weak MB fluorescence signal in the membrane contour (Fig. 1). Thus, a certain amount of  $^1\text{O}_2$  may be also produced in the membrane. We measured the partition coefficient of MB on both PC liposomes (see experimental part and the Supporting Material). The results show a small difference in  $K_b$  values that amounted to  $K_b = 34 \pm 6 \text{ M}^{-1}$  for DOPC and  $K_b = 27 \pm 5 \text{ M}^{-1}$  for POPC. Therefore, such

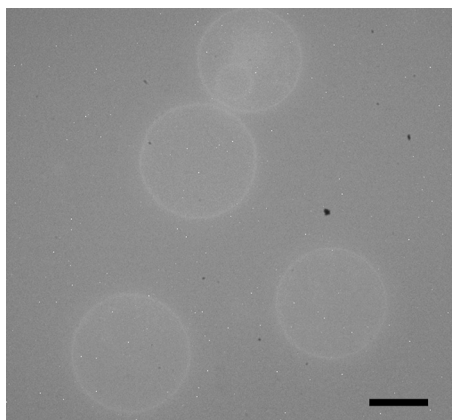


FIGURE 1 Fluorescence microscopy (665 nm) of DOPC giant vesicles dispersed in MB solution (30  $\mu\text{M}$ ). The fluorescence of MB is evidenced in solution as well as on the vesicles, denoting the adsorption of the compound on the lipids membrane. Bar spans 20  $\mu\text{m}$ .

a small difference does not bring about any further contribution to the amount of singlet oxygen generated in the DOPC in respect to the POPC membranes.

Fig. 2 shows typical morphological changes on the lipid membrane of DOPC or POPC giant vesicles dispersed in MB aqueous solutions and submitted to continuous photoirradiation (665 nm). Original spherical vesicles, exemplified in picture (a), remain physically stable as far as there is no singlet oxygen being produced in the solution. However, by submitting the observed vesicles to direct MB photoactivation, the lipid bilayer starts to increase in area and fluctuates after short periods of time at such extent that buds are released (b and c), inward buds (d) that may be related to invaginations (e) appear, eventually transient microholes that open (f) and close (g) on the membrane during a few seconds take place without disrupting the vesicles, followed by loss of membrane phase contrast (h). The speed and extent of the membrane physical damage depend strongly on the MB concentration in the outer vesicles solution. By turn, it must be related to the concentration of oxidative species nearby and in the membrane that are produced by photoirradiation, being capable to trigger some kind of photooxidative reaction with the phospholipids of the membrane bilayer. In particular, it is well known that  $^1\text{O}_2$  interacts with the double bond(s) on the acyl tail(s) of the unsaturated phospholipids promoting lipid hydroperoxidation. Interestingly, previous studies focusing on the photoresponse of GUVs containing porphyrin-based photosensitizers, which were incorporated into the lipid bilayer, evidenced an increase in the membrane area followed by buds emission due to the accumulation of lipid hydroperoxides, without loss of membrane contrast (23,28). Noteworthy, experiments performed on GUVs composed of saturated lipids did not show any morphological change in response to photoirradiation (23), demonstrating that, indeed, oxidative reaction is triggered by the attack of  $^1\text{O}_2$  to the chain double bond.

Therefore, by observing the photodamage of vesicles for long periods of time, besides the large membrane disturbances described previously, the vesicles behavior may be summarized to the following main events: 1), vesicles are spherical and apparently stable at the beginning; 2), vesicles start to flicker and the previously described behaviors may take place depending on MB concentration; 3), vesicles recover spherical shape and the membrane fluctuates less than before irradiation, followed by a decrease of the vesicle optical contrast; 4), slowly the vesicle loses completely the contrast. Such contrast loss evidences the traffic of fluids from the core of the vesicle to the external environment, and vice versa, because the refractive index of sucrose solution in the vesicles core differs from the glucose outer solution. Indeed, the loss of contrast denotes that both internal and external solutions are being homogenized. In this way, pores of at least 1 nm diameter must be formed in the lipid bilayer and allow sugar traffic. Therefore, pores formation

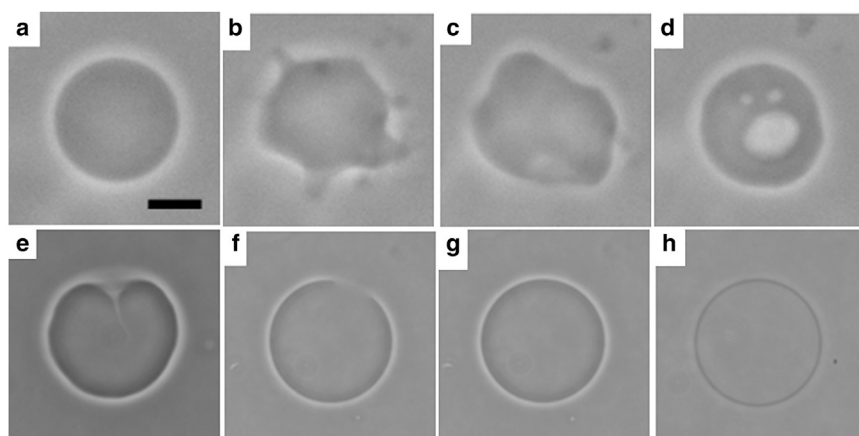


FIGURE 2 Phase contrast optical microscopy of time running sequences (*in seconds*) of the damage on giant vesicles membrane by photoactivation of MB (665 nm; 40  $\mu\text{M}$ ): (a) 01 s: stable vesicle; (b) 104 s, and (c) 108 s: vesicle flickers, buds release; (d) 138 s, and (e) 162 s: invaginations; (f) 191 s: large transient hole opens the membrane; (g) 193 s: apparent recover of stability; (h) 246 s: loss of phase contrast. Bar spans 20  $\mu\text{M}$  for all snapshots. See text for more details.

on the membrane is one of the prominent physical consequences of POPC and DOPC peroxidation promoted by photoirradiation of MB at concentrations up to 40  $\mu\text{M}$ .

In what follows, we evaluated the loss of contrast of individual POPC and DOPC vesicles by integration of the gray level profiles of the phase contrast microscopy images using ImageJ Launcher. Fig. 3 *a* shows a half POPC giant vesicle, with close to 20  $\mu\text{m}$  of diameter, cut over its equator before photoirradiation and after completely losing contrast. The gray level intensity has been obtained over the equator for both images (Fig. 3 *b*), and it shows high positive peaks be-

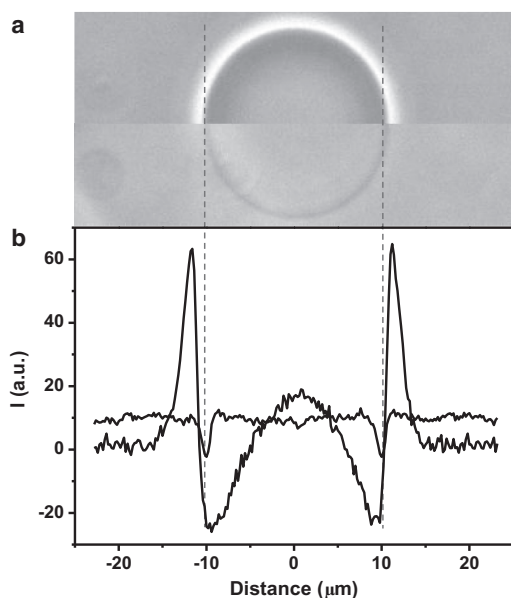


FIGURE 3 (a) Phase contrast microscopy of a giant vesicle showing the phase contrast decay by the action of photoactivated MB (at 665 nm). The vesicle snapshot is cut over its equator to show the difference before and after losing contrast. (b) Comparison of the intensity profiles across the equator. In this graph, the y axis measures gray levels and the x axis corresponds to  $\mu\text{m}$  in the above images; the higher intensity curve measures the gray levels in the high phase contrast condition and the lower intensity curve (intentionally displaced up to the zero average) measures the gray levels after completely losing the contrast.

side negative ones for the vesicle before irradiation, relative to the background of the image. These peaks are symmetric with respect to the vesicle center and correspond to the gray level difference of the maximal contrast, right over the vesicle membrane as expected. During contrast loss, the same peaks decrease in intensity and when the contrast is completely lost, only small negative peaks remain corresponding to the dark gray level, relative to the background, of the vesicle membrane.

In this manner, the relative intensity of contrast decay has been determined during photoirradiation for the two lipids studied herein by measuring the intensity of the positive peak at every few elapsed seconds. Fig. 4, *a* and *b*, show the results obtained for POPC and DOPC vesicles, respectively, dispersed in MB aqueous solution. In the case of POPC, the first curve on the left corresponds to the sample with 40  $\mu\text{M}$  MB, revealing that the pore opening starts at around 3 min of continuous illumination and the complete loss of contrast takes place within <2 min. By decreasing the MB concentration to 30 and 20  $\mu\text{M}$ , the loss of contrast took longer irradiation times around 13 and 18 min to initiate, respectively. For 10  $\mu\text{M}$  MB, it is evidenced that contrast was kept almost equal to the one before irradiation during some time. Afterward, the contrast intensity decreased in a similar way also for this concentration, i.e., sudden and during the last minutes of irradiation, which anticipate the complete loss of contrast.

A similar behavior was also observed for DOPC vesicles (Fig. 4 *b*). The relative intensities decreased faster and were sudden for higher concentrations of MB and took longer for the lower concentrations similar to the POPC results. Noteworthy, the irradiation times necessary to induce membrane pore formation were relatively shorter than those observed for POPC GUVs at the same MB concentration. Therefore, the mechanism of pore formation for DOPC GUVs is faster than that observed for POPC-based membranes for the same rate of singlet oxygen production. Thus, the difference in the structural characteristics of the phospholipids is, indeed, playing an important role in the oxidation process.

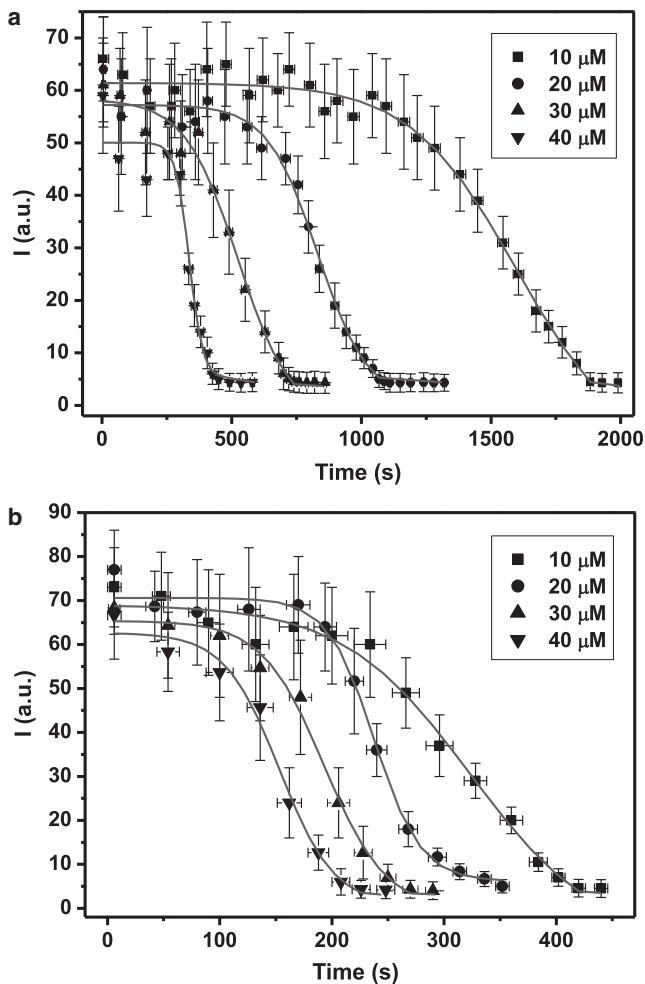


FIGURE 4 Profiles of contrast decay of POPC (a) and DOPC (b) giant vesicles for increasing concentrations of MB, as indicated in the inserted legends. Each point corresponds to the average of at least five vesicles and the uncertainty is represented by the error bar. Thick lines correspond to the best fitting of Eq. 1 to the experimental data.

### Electro-deformation of giant vesicles

It is further considered that a critical amount of phospholipids has to undergo oxidation to trigger the pores formation in the membrane (8,9). In seeking to estimate this amount of oxidized phospholipids on the vesicles, we have applied electro deformation of giant vesicles. As described elsewhere (23,32), in the presence of an AC field, lipid vesicles assume oblate or prolate shapes, with their symmetry axis lying parallel to the electric field, depending on the field frequency and conductivity ratio between the inner and outer solution. As described in the experimental part, to perform this experiment, vesicles were grown with the addition of a small amount of NaCl and later dispersed in a salt free solution. In this way, the conductivity of the inner solution was higher in respect to the outer solution and, hence, the AC field induced prolate deformation of the vesicles lying between two electrodes.

Systematically, spherical and unilamellar vesicles were initially submitted to the AC field until reaching the maximal observed prolate deformation that corresponds to the exposition of the usual hidden surface area due to thermal fluctuations. Such change in morphology under the electric field took around 1 min in average. The maximal area increase of the vesicles before irradiation lies around 2% for POPC and DOPC. The photoirradiation of MB was then started under the same AC field. At this point vesicles stretched, assuming a more elongated prolate shape, and the largest axis of the vesicles increased, whereas the smallest axis decreased with time keeping a constant volume. The sequence of the ongoing events is shown in Fig. 5 as an example. The additional vesicles stretching under photoirradiation denotes the increase in surface excess area of the phospholipids membrane that results from lipid peroxidation (23) without changing the inner conductivity (32). It has to be pointed out that the weak AC field applied here (10 V) is not enough for itself to stretch the bilayer at the molecular level (23,31). Thereby, all the area excess observed is related to the response of the membrane to photoirradiation.

Furthermore, the prolate deformation (Fig. 5 b) of the vesicles submitted to the AC field under irradiation was temporary. We note that the period of time that the vesicles remained with a prolate shape was related to the concentration of MB in the vesicle outer solution as well as to the structural features of the lipid (see Fig. 6). Basically, the membrane stretching was observed during the first seconds of irradiation. Later, the vesicles gradually recovered the spherical shape (Fig. 5 c) followed by optical contrast loss (Fig. 5 d).

It is well known in biological membranes that changes in the membrane lipid composition can lead to geometrical defects in the lipid packing. It has been recently shown that the introduction of conic lipids into flat bilayers induces chemical defects, where hydrocarbon chains are accessible to the solvent, and geometrical defects that give rise to voids deeper than the glycerol backbone (33). In our case, PC is a cylindrical lipid, but the peroxidation process generates new chemical structures of oxidized phosphatidylcholines (7,8); therefore, the sequence of events shown in Fig. 5, c and d, may suggest that, under an oxidative stress, oxidized lipids initially promote defects in the lipid packing. Such defects may facilitate the passage of small molecules as the ions of  $\text{Na}^+$  and  $\text{Cl}^-$  from the inner to the outer solution, until the conductivity of both solutions is equilibrated. In this situation, the vesicle recovers the spherical shape (32). One can thus speculate that the opening of hydrophilic transient pores takes place due to the formation of lipid packing defects. Afterward, when a sufficient amount of lipids is oxidized, pores in the membrane are generated, which then allow the traffic of the sugars resulting in membrane contrast loss (Fig. 5 d).

The increase in the relative surface area of the vesicles was here evaluated during the first seconds of irradiation,

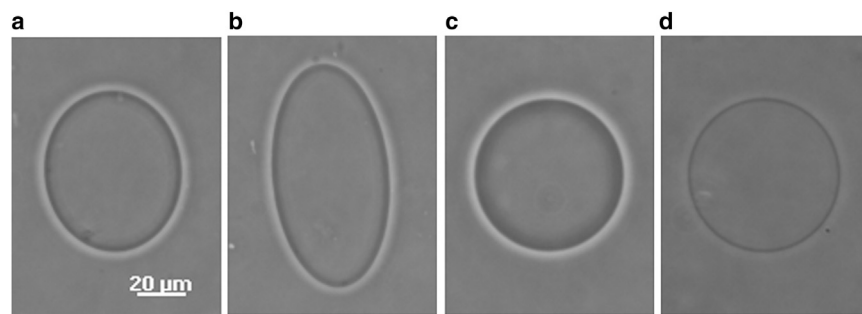


FIGURE 5 Phase contrast microscopy snapshots of the typical giant vesicles behavior under AC electric field (10 V, 1 MHz) and photoactivation of MB (665 nm) in the solution. Sequentially, the electric field induces prolate deformation in the absence of irradiation (*a*); under irradiation: the vesicles elongate further to the electric field direction reaching a maximum elongation (*b*), followed by a recovering of the original spherical shape after some time (*c*); finally, the phase contrast is lost (*d*).

at the maximal observed stretching of the lipid bilayers, assuming that the vesicle shape is a prolate ellipsoid (23). The vesicle surface area was calculated in short intervals and Fig. 6 shows the results from POPC and DOPC GUVs. As it may be noticed, the relative area ( $\Delta A/A_0$ ,

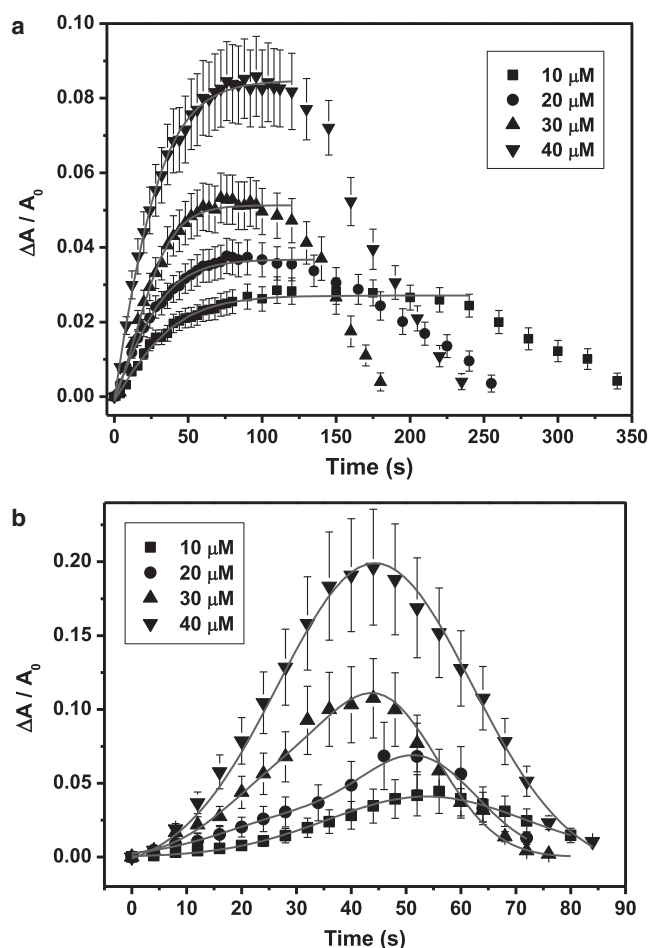


FIGURE 6 Surface area increase of GUVs under electro-deformation (10 V, 1 MHz) and photoactivation (665 nm) of different concentrations of MB in the solution, as indicated, for POPC (*a*) and DOPC (*b*) vesicles. Each point corresponds to the average of at least 10 vesicles and the uncertainty is represented by the error bar. The time sequence represents the scenarios displayed in Fig. 5, *a-c*. Solid curves are guide to the eye.

where  $A_0$  is the vesicle apparent surface area right before irradiation taking into account the excess of area of 2% due to initial hidden thermal fluctuations) increases for POPC vesicles in MB solution, reaching a maximal value that lasts sometime, followed by a decreasing of  $\Delta A$  until the original spherical shape is recovered with continuous irradiation.

On the other hand, for DOPC the relative surface area increased faster and reached higher values, in comparison to the ones for POPC. After reaching a maximal surface area, the prolate shape diminished gradually in extension, also leading to the recovering of the original spherical shape of the vesicles in a few seconds.

## DISCUSSION

### Lipids peroxidation

Peroxidation modifies the structural characteristics of the phospholipids that lead to remarkable alterations on molecular organization, molecular diffusion, and composition of the vesicles membrane. Lipid chains may assume new conformations requiring an increase in area per lipid (7,23), and eventually chain cleavage occurs due to the propagation of the peroxidation reaction. Chain cleavage opens the possibility of generating several truncated byproducts as ketones, aldehydes, or carboxylic acids (3,8,9). However, the only well-characterized process is the formation of lipid hydroperoxides. The exact molecules that are formed after this initial step still await experimental evidence.

We have shown that a certain amount of MB is located in the membrane (Fig. 1), with similar  $K_b$  values for DOPC and POPC. Thus, the differences in the rates of surface area increase between both vesicles, which were submitted to the same range of MB concentrations and irradiation conditions, are related to the number of unsaturation on the lipids acyl tails and denote a diverse molecular dynamic because of the oxidative process. First, it has to be pointed out that the average maximal area of the vesicles submitted to AC field observed before irradiation is around 2% for POPC and DOPC. The small area increase induced by AC field must be related to the degree of deformation that results from vesicles excess area, which is similar to experiments

of aspiration with micropipettes performed in the low tension regime (34). However, during irradiation, surface area increases to around 8% for POPC and around 19% for DOPC vesicles dispersed in 40  $\mu\text{M}$  MB solution, as evidenced in Fig. 6, after subtracting the previously mentioned excess area.

It is known that the reaction between singlet oxygen and lipid  $\pi$  bonds produces primarily hydroperoxides (35). Due to its hydrophilic character, it is shown that this group can migrate to the bilayer surface (7,23) promoting an increase in the average surface area, as schematically shown by Riske et al. (23). The larger area per lipid, due to the accumulation of hydroperoxide in the membrane, conducts to the morphological changes of the vesicles as observed herein and elsewhere (23,36), without membrane disruption or permeability increase.

Wong-Ekkabut et al. (10) estimated the amount of area increase caused by formation of lipid hydroperoxides using molecular dynamics simulations. Extrapolation of the simulations data shows that the area of one lipid containing an unsaturated chain may increase from 65 to 75  $\text{\AA}^2$  with the formation of hydroperoxide, hence an increment of 15%. A recent micropipette study has confirmed this increment for 100% fully hydroperoxidized POPC membrane (G.Weber, T.Charitat, M.Baptista, et al., Unpublished). Noteworthy, such GUVs did not present optical phase contrast lost or pore opening. Applying such estimative to the gain of surface area of our vesicles (15%), it turns out that for the POPC vesicles in MB solution the average maximal surface area increase of 8% corresponds to the hydroperoxidation percentage of phospholipids of 53% at 80 s of continuous irradiation. It corresponds, indeed, to a weighty amount of oxidation denoting the high quantum yield of singlet oxygen production by photoirradiating MB.

However, it may not be assumed that a larger amount of lipids, over the 53% determined previously, avoids hydroperoxidation after 80 s of irradiation. Indeed, during longer periods of irradiation one may reach 100% of hydroperoxidation. In this manner, our results suggest that, although hydroperoxidation increases the surface area, a generation of other oxidized lipids in the membrane may conduct to surface area reduction, hindering the determination of the 100% of hydroperoxidation. Of note, the apparent decrease of surface area of POPC over 80 s (Fig. 6) must be related to the formation of lipid packing defects and nanopores on the vesicles membrane, which allow ions to release from the GUV inner compartment to the outer solution. As a consequence, the applied electric field has no effect on the membrane that recovers its spherical shape.

Now comparing to DOPC, besides molecular morphology, electronic characteristics may be considered as an important feature to justify the quicker peroxidation of DOPC, taking into account that the acyl tails of this lipid bear four  $\pi$  orbitals forming two  $\pi$  bonds each. Indeed, the unsaturations are located between the 8th and 9th atoms

of carbon on both tails. Such a feature creates an increased localized electronic environment, e.g., the close position of the  $\pi$  bonds leads to an electronic repulsion between them. However, it creates at the same time an attractive electronic environment for reactive species as singlet oxygen. The electron donor capacity is thus higher on DOPC membrane in comparison to POPC membrane.

On the other hand, for DOPC vesicles we revoke to calculate the amount of hydroperoxide. First, as the membrane surface area increase shows a large variation (Fig. 6), along with an abrupt drop after reaching a maximal, it is not certain whether the membrane is affected mainly by hydroperoxidation or if various molecular modifications of the lipids under excessive disturbances caused by reorientations of the acyl tails are ruling the membrane characteristics. Wan-Yu Tai et al. (37) have observed, for instance, a strong correlation between the modification of DOPC structure as a result of oxidation and the alteration of the vesicles membrane fluidity. Herein, our microscopy observations denote a high increase of the membrane fluctuations during the first seconds of irradiation that coincide with the raise of the membrane area. All the molecular disturbances favor further the membrane permeability increase that is characterized by the loss of membrane optical contrast due to sugar traffic between the inner and outer GUV solution as discussed below.

## Pores formation

Molecular reorientation that results from peroxidation enables the upsurge of pores on the vesicles membrane. As discussed before, it is accepted that the oxidized lipid chains tilt toward the polar region of the membrane increasing the area per lipid (23). This conformation weakens the lateral interactions between headgroups, raising the average distance between them, which consequently permits solution traffic. The hydrophilic headgroups follow the water molecules that enter the membrane, leading to a direct interaction between the headgroups located in the opposite leaflet, allowing in this manner the opening of a hydrophilic pore (38).

Our results show that the physical damage caused on the phospholipid membrane, which ends up in pore opening, is tuned by the concentration of MB. The way the kinetics of loss of contrast depends on the MB amount is different for the POPC and DOPC vesicles. As Fig. 4 evidences, POPC vesicles respond to oxidative stress slower than do DOPC vesicles. To further evaluate the contrast decay as a function of the irradiation time,  $t$ , we have applied a Boltzmann equation to the curves shown in Fig. 4, *a* and *b*, as

$$I = A_2 + (A_1 - A_2)/(1 + \exp((t - \tau)/d\tau)), \quad (1)$$

with  $A_1$  and  $A_2$  the upper and lower limits;  $\tau$  expresses the mean time, and  $d\tau$  the characteristic time of loss of optical contrast.

Fig. 7 *a* shows  $\tau$  values as a function of MB concentration. For POPC vesicles, the loss of contrast occurs after a delay inversely proportional to MB concentration (exponent  $-1.0$  from the fitting to the data displayed in Fig. 7 *a*). On the other hand, the DOPC vesicles loss of contrast obeys a more unusual scaling behavior with an exponent  $-0.5$  of the same quantity. This suggests that membrane damage is the consequence of rather complex and nonuniversal kinetic mechanisms.

The characteristic time  $d\tau$  from the POPC GUVs to completely lose its contrast also decreases with the increase of the amount of MB (Fig. 7 *b*). Intriguing, the characteristic time  $d\tau$  for DOPC is practically constant around 10 s for MB concentrations  $>10 \mu\text{M}$  (Fig. 7 *b*). Moreover, it becomes closer to that found for POPC vesicles at the largest MB amount of  $40 \mu\text{M}$ .

Based on these observations, we put forward a possible scenario for membrane damage that may account for both regimes as two limiting cases. We assume first that the

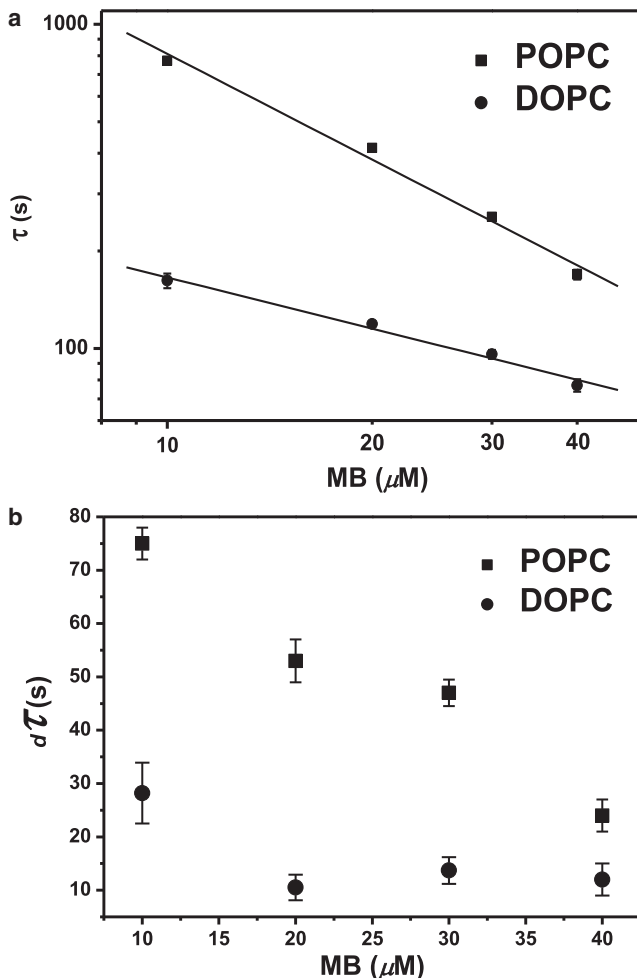


FIGURE 7 Mean time  $\tau$  (*a*) and characteristic time  $d\tau$  of membrane permeabilization (*b*) of POPC and DOPC giant vesicles for increasing concentrations of MB.

loss of contrast results from a loss of membrane integrity associated with pores formation, and we assume that pores open when a sufficiently large concentration of oxidized lipids occurs at some location in the membrane. On the other hand, we make the reasonable assumption that lipid oxidation takes place with uniform and constant rate  $\alpha$ , itself proportional to the light beam intensity and photosensitizer concentration. In our case, the light intensity is constant for all experiments. Therefore,  $\alpha$  is proportional to MB concentration.

If oxidized species segregate from nonoxidized ones, the initial nucleation of a seed rich in oxidized species will be followed by a diffusion-limited growth regime, in which the number of oxidized lipids increases as  $\alpha Dt^2$ ,  $D$  being the diffusion constant (see the Supporting Material, entry 2). We then argue that pores open massively when the number of lipids in each domain reaches a critical value  $n_c$ , resulting in the observed loss of contrast. Under this mechanism, membrane degradation takes place around a mean time  $\tau \propto (\alpha D)^{-0.5}$  (Eq. 9 in the Supporting Material).

The picture is different, however, if for any reason the growth of oxidized rich nanodomains is slow, or if the number of such nucleated nanodomains is large, as would be the case, for instance, in a homogeneous nucleation process. The nanodomains would then start competing with each other for the oxidized molecules that are formed independently at a constant rate  $\alpha$ . The expected law of growth in this case turns out to be linear in time (see the Supporting Material, entry 2), and independent from the diffusion constant  $D$ . The time necessary to reach the threshold  $n_c$  now scales as  $\tau \propto \alpha^{-1}$  (Eq. 11 in the Supporting Material). Thus, in this regime, pores open when the overall fraction of oxidized lipid reaches a certain value, as one would have intuitively expected.

Therefore, based on this model, the reason why DOPC falls in the first category and POPC falls in the second category could be traced back to a stronger repulsion between oxidized and nonoxidized species, the growth of oxidized rich domains being slower or suppressed in the POPC case. Of course, these arguments do not form a precise theory for pore formation, but only a schematic mechanism. More should be known about the membrane structural changes induced by oxidation before such a theory could be attempted. Furthermore, we did not consider the double leaflet structure and need of the pores to span across the full length of the bilayer. Future work is necessary to encompass the full range of possible kinetics mechanisms associated with domain formation with a species that is created at the same time it diffuses and migrates toward the prepore domains.

## CONCLUSION

Both membranes studied herein, i.e., GUVs made either of POPC or DOPC, presented important morphological and

structural changes due to the photosensitization reactions. Areas increase, and contrast loss quantified by decrease in refractive index gradient and electrochemical gradient across the membranes, show to be proportional to MB concentration in both cases. However, the mean time of vesicle degradation varied with the square root of the MB concentration in the case of DOPC-made vesicles and linearly in the case of POPC vesicles. Knowing that all photophysical variables are similar for these two lipids (MB efficiency, MB membrane binding) we attributed this difference to the way the oxidized lipids organize themselves in the membrane. In the case of DOPC the nucleation process of oxidized species follows a diffusion-limited growth regime and in the case of POPC a homogeneous nucleation process. Equations were derived and fit to the experimental data giving confidence to the observation. This information is important because it shows that the outcome of a photo-induced oxidation reaction in the membrane vicinity is critically dependent on the type of lipid that is present within the membrane.

Furthermore, we were able to characterize both the increase in membrane surface area and the upsurge of sodium chloride permeability, highlighting a new, to our knowledge, application of the electro-deformation methodology applied to GUVs.

## SUPPORTING MATERIAL

One figure, eleven equations, and supporting data are available at [http://www.biophysj.org/biophysj/supplemental/S0006-3495\(13\)05716-0](http://www.biophysj.org/biophysj/supplemental/S0006-3495(13)05716-0).

This work was supported by grant No. 2012/50680-5, São Paulo Research Foundation (FAPESP). O.M. thanks FAPESP for a postdoctoral fellowship (process: 2010/18163-5). This work is also part of a bilateral agreement USP-Cofecub (No.: 2010.1.1049.43.9). R.I. and M.S.B. also acknowledge Conselho Nacional de Pesquisa (CNPq) for research fellowships.

## REFERENCES

- Levsikaya, A., O. D. Weiner, ..., C. A. Voigt. 2009. Spatiotemporal control of cell signalling using a light-switchable protein interaction. *Nature*. 461:997–1001.
- Shapiro, M. G., K. Homma, ..., F. Bezanilla. 2012. Infrared light excites cells by changing their electrical capacitance. *Nat. Commun.* 3:736-1–736-7.
- Fruhwrth, G. O., A. Loidl, ..., A. Hermetter. 2007. Oxidized phospholipids: from molecular properties to disease. *Biochim. Biophys. Acta*. 1772:718–736.
- Girotti, A. W. 1990. Photodynamic lipid peroxidation in biological systems. *Photochem. Photobiol.* 51:497–509.
- Niziolek-Kierecka, M., A. Pilat, ..., A. W. Girotti. 2010. Apoptosis-accommodating effect of nitric oxide in photodynamically stressed tumor cells. *Photochem. Photobiol.* 86:681–686.
- Huber, J., A. Vales, ..., N. Leitinger. 2002. Oxidized membrane vesicles and blebs from apoptotic cells contain biologically active oxidized phospholipids that induce monocyte-endothelial interactions. *Arterioscler. Thromb. Vasc. Biol.* 22:101–107.
- Stemmer, U., Z. A. Dunai, ..., A. Hermetter. 2012. Toxicity of oxidized phospholipids in cultured macrophages. *Lipids Health Dis.* 11:110.
- Borst, J. W., N. V. Visser, ..., A. J. W. G. Visser. 2000. Oxidation of unsaturated phospholipids in membrane bilayer mixtures is accompanied by membrane fluidity changes. *Biochim. Biophys. Acta*. 1487:61–73.
- Schnitzer, E., I. Pinchuk, and D. Lichtenberg. 2007. Peroxidation of liposomal lipids. *Eur. Biophys. J.* 36:499–515.
- Wong-Ekkabut, J., Z. Xu, ..., L. Monticelli. 2007. Effect of lipid peroxidation on the properties of lipid bilayers: a molecular dynamics study. *Biophys. J.* 93:4225–4236.
- Beranova, L., L. Cwiklik, ..., P. Jungwirth. 2010. Oxidation changes physical properties of phospholipid bilayers: fluorescence spectroscopy and molecular simulations. *Langmuir*. 26:6140–6144.
- Jurkiewicz, P., A. Olżyńska, ..., M. Hof. 2012. Biophysics of lipid bilayers containing oxidatively modified phospholipids: insights from fluorescence and EPR experiments and from MD simulations. *Biochim. Biophys. Acta*. 1818:2388–2402.
- Conte, E., F. M. Megli, ..., E. Bordignon. 2013. Lipid peroxidation and water penetration in lipid bilayers: a W-band EPR study. *Biochim. Biophys. Acta*. 1828:510–517.
- Stemmer, U., and A. Hermetter. 2012. Protein modification by aldehydophospholipids and its functional consequences. *Biochim. Biophys. Acta*. 1818:2436–2445.
- Tardivo, J. P., L. H. Paschoal, ..., A. D. Giglio. 2006. New photodynamic therapy protocol to treat AIDS-related Kaposi's Sarcoma. *Photomedicine and Laser Surgery*. 24:528–531.
- Tardivo, J. P., M. Wainwright, and M. S. Baptista. 2012. Local clinical phototreatment of herpes infection in São Paulo. *Photodiagn. Photodyn. Ther.* 9:118–121.
- Wainwright, M., and K. B. Crossley. 2002. Methylene Blue—a therapeutic dye for all seasons? *J. Chemother.* 14:431–443.
- Gabrielli, D., E. Belisle, ..., M. S. Baptista. 2004. Binding, aggregation and photochemical properties of methylene blue in mitochondrial suspensions. *Photochem. Photobiol.* 79:227–232.
- Kessel, D. 1990. In *Photodynamic Therapy of Neoplastic Disease, Vols. 1 and 2*. CRC, Boston, MA.
- Junqueira, H. C., D. Severino, L. G. Dias, ..., 2002. Modulation of methylene blue photochemical properties based on adsorption at aqueous micelle interfaces. *Phys. Chem. Chem. Phys.* 4:2320–2328.
- Severino, D., H. C. Junqueira, ..., M. S. Baptista. 2003. Influence of negatively charged interfaces on the ground and excited state properties of methylene blue. *Photochem. Photobiol.* 77:459–468.
- Caetano, W., P. S. Haddad, ..., C. M. Marques. 2007. Photo-induced destruction of giant vesicles in methylene blue solutions. *Langmuir*. 23:1307–1314.
- Riske, K. A., T. P. Sudbrack, ..., R. Itri. 2009. Giant vesicles under oxidative stress induced by a membrane-anchored photosensitizer. *Biophys. J.* 97:1362–1370.
- Heuvingh, J., and S. Bonneau. 2009. Asymmetric oxidation of giant vesicles triggers curvature-associated shape transition and permeabilization. *Biophys. J.* 97:2904–2912.
- Girotti, A. W. 1998. Lipid hydroperoxide generation, turnover, and effector action in biological systems. *J. Lipid Res.* 39:1529–1542.
- Wang, Z. 2010. Hock Rearrangement. *Comprehensive Organic Name Reactions and Reagents*. John Wiley, Hoboken, NJ.
- Megli, F. M., L. Russo, and K. Sabatini. 2005. Oxidized phospholipids induce phase separation in lipid vesicles. *FEBS Lett.* 579:4577–4584.
- Haluska, C. K., M. S. Baptista, ..., R. Itri. 2012. Photo-activated phase separation in giant vesicles made from different lipid mixtures. *Biochim. Biophys. Acta*. 1818:666–672.
- Stewart, J. C. M. 1980. Colorimetric determination of phospholipids with ammonium ferrioxalate. *Anal. Biochem.* 104:10–14.
- Angelova, M. I., and D. S. Dimitrov. 1986. Liposome electroformation. *Faraday Discuss. Chem. Soc.* 81:303–311.

31. Riske, K. A., and R. Dimova. 2005. Electro-deformation and poration of giant vesicles viewed with high temporal resolution. *Biophys. J.* 88:1143–1155.
32. Aranda, S., K. A. Riske, ..., R. Dimova. 2008. Morphological transitions of vesicles induced by alternating electric fields. *Biophys. J.* 95:L19–L21.
33. Vamparys, L., R. Gautier, ..., P. F. Fuchs. 2013. Conical lipids in flat bilayers induce packing defects similar to that induced by positive curvature. *Biophys. J.* 104:585–593.
34. Evans, E., and W. Rawicz. 1990. Entropy-driven tension and bending elasticity in condensed-fluid membranes. *Phys. Rev. Lett.* 64:2094–2097.
35. Brault, D., C. Vever-Bizet, and T. Le Doan. 1986. Spectrofluorimetric study of porphyrin incorporation into membrane models—evidence for pH effects. *Biochim. Biophys. Acta.* 857:238–250.
36. Reference deleted in proof
37. Tai, W. Y., Y. C. Yang, ..., I. Liao. 2010. Interplay between structure and fluidity of model lipid membranes under oxidative attack. *J. Phys. Chem. B.* 114:15642–15649.
38. Cwiklik, L., and P. Jungwirth. 2010. Massive oxidation of phospholipid membranes leads to pore creation and bilayer disintegration. *Chem. Phys. Lett.* 48:99–103.